The Role of Morphological Computation of the Goat Hoof in Slip Reduction

Sara-Adela Abad[1], Nantachai Sornkarn[1] and Thrishantha Nanayakkara[1]

***Abstract*—The remarkable ability of goats to maintain stability during climbing cliffs or trees provides a valuable opportunity to understand some of the secrets of stable legged locomotion on unstructured terrains. This paper, for the first time, presents analytical and experimental explanations as to how the morphological computation at the goat hoof makes a significant contribution to slip reduction on both smooth and rough surfaces. We conducted experiments using a laboratory made hoof and compared its dynamic behavior against a rounded foot. We recorded forces and position of the hoof to analyze the effect of its shape and the individual contributions from 3-joints in the hoof on the work required to slip. Results state that the work required to move the hoof is more than 3 times that required to move a rounded foot. Additionally, the variables in the transient state are affected not only by the number and type of joints but also by the interaction with the environment. These findings promote the development of new types of feet for robots for all terrain conditions with greater stability and less control complexity.**

I. Introduction

Legged locomotion offers many advantages such as the opportunity to come into contact with a rough terrain at selected locations, ability to control the direction of contact forces, and deform soft soil to aid forward movement. However, the punctuated forces at each foot-ground collision produce uncertainty of slip, and the piece-wise non-linear interaction dynamics experienced during each collision [1] makes walking harder than many other modes of locomotion.

Technology on robotic legged walkers has made significant advances in the recent past starting from simple passive dynamic walking experiments [2] in 1980's to the Big Dog [3] and the LittleDog [4] developed by Boston Dynamics. Though they have demonstrated exceptional capabilities in outdoor locomotion, they use basic rounded feet. We predict that a better foot design will help to improve their stability and energy efficiency on unstructured and slippery terrains.

Some other attempts to develop legged walkers include Dagsi Whegs™[5], RHex [6], MSROX [7], and IMPASS [8]. RHex in particular follows the biological inspiration from cockroaches that there is no defined border separating the foot and the rest of the leg. However, the dynamic analysis of RHex legs in the form of an elastic template shows the importance of the role of morphological computation in the dynamic performance of the walker. Throughout this paper, the notion - *morphological computation* - refers to the computations done by bodily circuits in contact with the environment. A good example is demonstrated when the body of a dead trout is placed against a stream of turbulent water, the passive interaction water-body creates vortexes that propel the dead fish against the stream [9]. This phenomenon cannot be seen in other objects of similar weight like a hard stick or a soft piece of cloth.

All other larger walkers use simple foot designs that do not demonstrate morphological computational capabilities of their biological counterparts like the hoofs of animals known for having an ecological niche in muddy and hilly terrains. For instance, IMPASS is stable due to its whegs that are rimless wheels with individually actuated spokes; but its control can be more complex than that of RHex. This increases the power consumption for uneven terrain. This is clearly illustrated in Dagsi Whegs™[5]. It requires the same power for walking over three hours on relatively level terrain as for climbing for 45 minutes. Therefore, power consumption, control complexity, and stability remain as the main limitations.

In this paper we introduce a novel multibody compliant robotic foot inspired by the hoof of goats for terrains with high variability. It has the following advantages: *a*) it has two interdigital ligaments (distal and proximal) that allow spreading the two halves of the hoof; this increases the likelihood of grabbing something rough or hold on a crack *b*) when walking downhill, the higher compliance of the hoof in the lateral direction leads to a larger slip dissipation orthogonal to the direction of walking, providing a natural stabilizing effect. *c*) goats have a rough flexible traction pad in the lower part of the hoof which slightly pasts the nail; it is a shock absorber that also generates a friction force due to its texture and its capability of impressing in any irregularity of the terrain *d*) an additional brake force is generated by the soil or rocks stuck between the claws[10]. Consequently, our minimalistic design embodies most of these benefits and exploits passive dynamics to ensure an improvement on the stability with a low energy cost and without increasing the control complexity.

In this research, we attribute the passive stabilizing effect of the hoof to its morphological computation in dynamic contact with the ground that changes the work required to slip along a fixed distance and the behavior of the forces f_y and f_z, the displacement y along Y, and the angles of the joints Θ, β, and γ (summarized in Table I) during the transient state.

Using this novel passive dynamic foot, we demonstrate that the work required to slide the hoof over two different substrates (soft and rough bricks) is more than 3 times that needed for a rounded foot, the common approach for robotic

The work described in this paper is supported in part by the Ecuadorian Government through SENESCYT and the U.K. Engineering and Physical Sciences Research Council (EPSRC) under Grants: EP/I028765/1 and EP/I028773/1.

[1]Sara-Adela Abad, Nantachai Sornkarn, Thrishantha Nanayakkara are with the Faculty of Natural and Mathematical Sciences, King/s College London, London, WC2R 2LS, UK (e-mail: sara.abad_guaman, nantachai.sornkarn, thrish.antha@kcl.ac.uk)

feet. Besides, results show that during the transient each joint has a different effect over the displacements and forces.

The rest of the paper is organized as follows: Section II provides a biological description of the goats' hoof and presents the design of our approach. Section III explains the methodology utilized to collect the data for the soft and rough terrain. Section IV presents and discusses the evolution of the position, forces, and work for each configuration described in the methodology. Then, Section V presents the conclusions and future work.

II. Biologically Inspired Foot

In nature there is a myriad of hoofed animals. They share similar features such as hoofs, pads, and bone structure that suits their ecological niches. For instance, camels avoid sinking their feet in sand by using their 2 toes whose contact area with the ground increases due to their broad foot pad that flattens with the weight and the absence of the proximal interdigital ligament [11] which facilitate spreading their wide toes. However, they are prone to injuries in rocky terrain. On the other hand, pigs that are commonly found in soft terrains have two straight hooves and 2 declaws (similar to those of the hoof illustrated in Figure 1(a) as III and IV, and II and V, respectively). All four are totally developed but their length is different. Declaws are smaller and higher than claws III and IV; therefore, they provide stability when the foot is sunk in the mud[12]. Nevertheless, among the ungulates, goats are well known for climbing trees and dams. The structure, size, and morphological computation of their hooves facilitates walking in terrain with high variability. Consequently, they are our biological inspiration to test the role of different morphological features in the hoof to increase the work required to slide the feet over two terrains.

A. Biological description of the hoof

Figures 1(a) and (c) illustrate the structure of the biological foot. They have cloven hoofs that are called toes or claws. These toes are covered with hard keratin whose front side ends in a tip which allows digging into the soil for walking uphill; additionally, mountain goats have a rough textured pad that is slightly projected over the nail to increase the friction with smooth surfaces and absorb shocks. The inter-digital ligaments facilitate their locomotion in uneven terrain because they increase the likelihood of a toe to stand over firm terrain; furthermore, when walking downhill the higher compliance of the hoof in the lateral direction leads to a larger slip dissipation orthogonal to the direction of walking, which provides a natural stabilizing effect. Moreover, the rocks or soil stuck in the inter-digital cleft provides an extra brake [10]. To join the phalanges with the metacarpals and to provide mobility of the claws in the different planes, there are three joints: fetlock (metacarpophalageal), pastern (proximal interphalangeal) and the coffin (distal interphalangeal) joint. The mobility of the bones is controlled by flexor and extensor tendons. However, this research intends to study the passive dynamics of the foot. Therefore, the minimalist design includes these three joints,

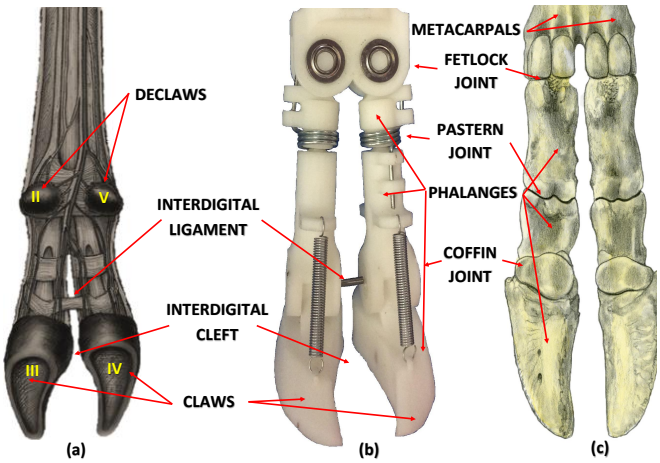

Fig. 1. Natural and constructed goats' feet. a) Ligaments and external view of the hoof. b) Biologically inspired foot. c) Bones of the foot (Courtesy: G. Constantinescu [13]). Two pairs of bearings were utilized for the fetlock (metacarpophalageal) joints, 2 sets of 3 bearings for the pastern joints (proximal interphalangeal), and 2 bearings for the coffin (distal interphalangeal) joints. To set up the default position of the claws to the front, a torsional spring was placed on the pastern joint. For emulating the inter-digital ligament, an extension spring was placed between the claws. Tendons, normally emulated with motors, have been represented using antagonistic springs in each claw. This allows passive control of its tension and extension movements without adding an extra-weight and energy consumption.

the distal interdigital ligament, the phalanges, and tendons are replaced by springs.

B. Modeling

To have a criterion to evaluate the effect of the joints while the foot is in contact with the ground, the static model of the system, illustrated in Figure 2(a), was derived. The parameters and variables are described in Tables I and II and the forces of the systems are: $\boldsymbol{F} = [0 \;\; f_y \;\; -f_z]^T$; $\boldsymbol{N}_3 = [0 \;\; 0 \;\; K_g l_g]^T$; and $\boldsymbol{F}_{r_3} = \left[-f_{r_x} \;\; -f_{r_y} \;\; 0\right]^T$. Additionally, we assume that the system is symmetric; therefore, $\boldsymbol{F}_{3/1} = -\boldsymbol{F}_{1/3} = f_{13}\left[-\sin\Theta \;\; -\cos\Theta\sin\phi \;\; \cos\Theta\cos\phi\right]^T$, $\boldsymbol{F}_{3'/1} = -\boldsymbol{F}_{1/3'} = \left[f_{13_x} \;\; -f_{13_y} \;\; f_{13_z}\right]^T$, and $l_{id} = l_{13}\sin\Theta - x$. Firstly, we balance the forces in the system to obtain:

$$f_{r_y} = 0.5 f_y \tag{1}$$

$$f_z = -2K_g l_g \tag{2}$$

After, applying equilibrium conditions at segment 01 we find:

$$\boldsymbol{F} = \boldsymbol{F}_{K_1/1} \tag{3}$$

Then, by balancing the forces at nodes we have:

$$f_y = 2f_{13}\cos\Theta\sin\phi \rightarrow f_{13} = \frac{f_y}{2\cos\Theta\sin\phi} \tag{4}$$

$$f_z = 2f_{13}\cos\Theta\cos\phi \tag{5}$$

$$-K_g l_g = f_{13}\cos\Theta\cos\phi \tag{6}$$

$$f_{r_x} + K_{id} l_{id} = f_{13}\sin\Theta \tag{7}$$

Replacing (4) in (5), (6), and (7) we obtain:

$$f_z = f_y \cot\phi \tag{8}$$

$$-K_g l_g = 0.5 f_y \cot\Theta \tag{9}$$

$$f_{r_x} = \frac{f_y \tan\Theta}{2\sin\phi} - K_{id}(l_{13}\sin\Theta - x) \tag{10}$$

Using (1), (9), and (10) in the relation $f_{r_x}^2 + f_{r_y}^2 = (\mu K_g l_g)^2$ we found:

$$f_y = \frac{2K_{id} l_{13}\sin\Theta - x}{\left[\frac{\tan\Theta}{\sin\phi} - \left(\mu^2\cot^2\phi - 1\right)^{1/2}\right]} \tag{11}$$

This establishes a proportional relation between K_{id} and f_y that was evaluated using the values presented in Table II. As Figure 2(b) shows, there is a critical point at $\Theta = 58.34$. Before this point the force required for the equilibrium of the system increases with K_{id} and Θ. After this point the system becomes unstable. Therefore, a force contrary to the direction of the movement has to be applied because claws tend to easily apart from each other.

TABLE I
ANALYZED VARIABLES

Description	Symbol	Units
Displacement of the foot along Y axis	y	mm
Force in the Y axis at point 0[1⋆]	f_y	N
Force in the Z axis at point 0[1⋆]	f_z	N
Position between the front and back of the claw[2⋆]	β	mm
Half the angle between the claws	Θ	°
Angle between the foot and axis Y	γ	°

[1⋆] 0 is the point of connection between the XY table and the feet.
[2⋆] The distance was calculated along the Z axis.

TABLE II
VARIABLES AND PARAMETERS OF THE MODEL AND SIMULATION

Variables / Parameters	Symbol	Value	Units
Displacement of the spring K_1	l_1	-	mm
Displacement of the spring K_{id}	l_{id}	-	mm
Displacement of ground	l_g	-	mm
Half the natural distance $3p$	x	-	mm
Mag. of the forces $\boldsymbol{F}_{K_3/1}$ and $\boldsymbol{F}_{K_{3'}/1}$	f_{13}	-	N
Normal Force at 3	$\boldsymbol{N}_3$	-	N
External force at 0 [1⋆]	$\boldsymbol{F}$	-	N
Friction Force between ground and claw	$\boldsymbol{F}_{r_3}$	-	N
Force of the spring K_1 over point 0	$\boldsymbol{F}_{K_1/0}$	-	N
Force of the spring K_1 over joint 1	$\boldsymbol{F}_{K_1/1}$	-	N
Force of the spring K_{id}	$\boldsymbol{F}_{K_{id}}$	-	N
Force from joint 3 to joint 1	$\boldsymbol{F}_{K_3/1}$	-	N
Force from joint 3' to joint 1	$\boldsymbol{F}_{K_{3'}/1}$	-	N
Static coefficient of friction	μ	1.7	
Angle between the foot and axis Z	ϕ	15	°
Stiffness of the interdigital spring[2⋆]	K_{id}	0.15	N/mm
Stiffness of the prismatic joint	K_1	363.63	N/mm
Stiffness of the ground	K_g	300	N/mm
Length from joint 1 to joint 3	l_{13}	110	mm

[1⋆] 0 is the point of connection between the XY table and the feet.
[2⋆] K_{id} has 3 values: $K_{id} = 0.05$[N/mm], $K_{id} = 0.15$[N/mm], and $K_{id} = 0.55$[N/mm]

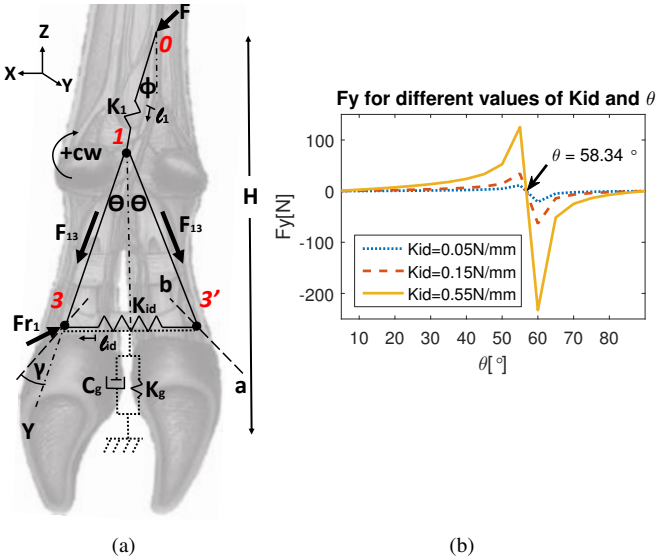

(a) (b)

Fig. 2. a) Diagram of the Mathematical model of the hoof. b) Evolution of Fy for different stiffness of the interdigital spring and Θ values. It illustrates a critic point at Θ_c=58.34[°]. Before this point f_y in the direction of the movement increases with K_{id} and Θ to keep the equilibrium. Conversely, after Θ_c, the system becomes unstable. Therefore, a force contrary to the direction of the movement has to be applied because claws tend to easily apart from each other.

C. Mechanical Design

As stated in Section I, the main limitation of robots for variable terrains are control complexity, power consumption, and stability. Therefore, a major challenge is to design a foot that passively adapts to the environment without affecting these parameters. To achieve our goal, the design is entirely comprised of passive elements and it was based on the claw of a mountain goat shown in Figure 3(c).

The hoof structure was constructed using a 3D printer with ABSplus as model material. Its total weight is 82.6g. Its height, illustrated in Figure 4(b), is 110mm, and the length of the claw is 55mm. The joints presented in Figure 1 were built using two stainless steel bearings of 6x12x3mm for the fetlock (metacarpophalangeal) joint, 3 stainless steels Metric Plain Bearing of 4x7x2.5mm for the pastern joints (proximal interphalangeal), and one 3D printed bearing for the coffin (distal interphalangeal) joint. To set up the default position of frontal end of the claws, torsional springs (PART NUMBER: LTMR100T 04 M and LTML100T 04 M for the left and right claws, respectively) were placed on the pastern joints. The inter-digital ligament was replicated by an extension spring. This facilitates the foot to get stuck even in small holes. Moreover, Figures 3(a) and (d) illustrate the antagonistic springs of the front and back of each claw that passively control its tension and extension movements. Hooves' shape was extracted from Figure 3(c). It exhibits the feet of a mountain goat taken in Ecuador. At the end, Figures 3(b),(d), and (e) exhibit the pad made of Ethylene-vinyl Acetate that is commonly used in slippers and sandals due to its low weight and moldability.

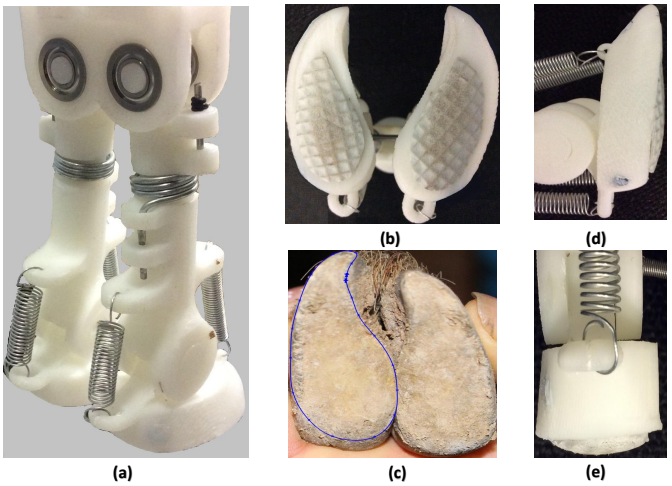

Fig. 3. Biologically inspired foot.a) General view: it illustrates the antagonistic springs on the front and back of each claw that passively control the tension and extension movements. b) Bottom view: each claw has a sole that is made of Ethylene-vinyl Acetate. It provides the same functionality to the claw as the rough textured pad does to the hoof. Its shape was designed using picture c). It exhibits the hooves of a mountain goat taken in Ecuador. Finally, d) the Lateral view and e) the Back view provides a better illustration of the slight projection of the pad over the nail.

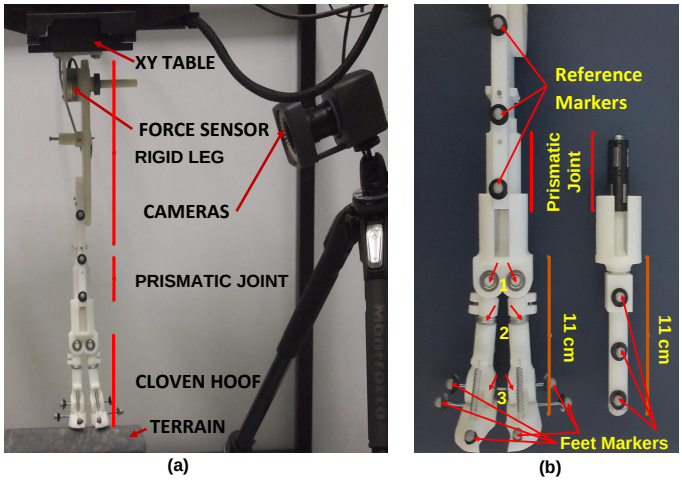

Fig. 4. Experiment setup. a) The foot is attached through the prismatic joint to the rigid leg while the force sensor couples this leg to the XY table that moves with a constant speed in the Y direction. 4 cameras were used to track the position of the markers of the claws. Additionally, a 5 seconds delay at the beginning and end of each trial together with three markers attached to the rigid leg were the reference to synchronize the data. The tested surface were a red house brick and a wood brick covered with black plain paper. b) 11 cm height feet utilized in the experiment. *Left:* Constructed hoof: It has 3 joints whose stiffness can be changed. It has an Ethylene-vinyl Acetate pad attached under each claw to increase the friction with the ground. *Right:* Rounded foot:it not only has the same length as the hoofed foot but also its contact area with the ground was covered with the same material of the pads of the hoof.

III. Experimental Methodology

Two experiments (one for each type of terrain) were conducted to analyze the effects of the type of feet, joint stiffness, and terrain on the work(stability) required to slide them. The speed was set constant and the position and forces during the transient and steady state were measured for feet combinations summarized in Table III during the experiments.

A. Experimental protocol

Figure 4 shows the the overview of the experimental setup. The foot is attached through a prismatic joint to the rigid leg. This joint contains the compression spring $K_1 = 363.63$N/mm for passively change in the normal force. The force sensor couples the rigid leg to the AEROTECH XY table type ANT130-160-XY-25DU-XY-CMS that moves with a constant speed of 10mm/second in the Y direction along the width of the bricks. The first tested surface was the smooth terrain (A). It was a wood brick covered with plain black paper whose length, width, and height were 20cm, 8.5cm, and 9cm, respectively. The second surface, named terrain (B), was a surface with a relatively high coefficient of friction. It was a red house brick whose length, width, and height were 19.8cm, 10cm, and 5cm, respectively. Four VICON Bonita B10 cameras (2 cameras located in the front of the hoof and 1 camera to each side of the foot) were used to track the position of the markers. The probed distance was the width of the bricks because feet were moved along this dimension. For synchronizing the position and the force data, a delay of 5 seconds at the beginning and end of each trial was set. Besides, three markers were attached to the rigid leg to have an additional synchronization reference.

B. Foot configuration

To identify the effect of passive dynamics on the work and the variables in Table I, the shape and joints' stiffness of the feet, presented in Figure 4(b), were changed according the 9 configurations summarized in Table III. Most of the joints were locked with clamps. Only, joint 3 that had antagonistic springs at the front and at the rear of the claw, whose stiffness are $K_f = 0.15$ N/mm and $K_b = 0.18$N/mm, was fasten with metallic screws whose distances were those of the antagonistic springs when the claw is perpendicular to the phalanges. Besides, an interdigital spring K_{id} was utilized to stabilize joint 1 when it is set free. Finally, to passively join the back ends of the claws in the last configuration, a piece of fabric with a length of 5 mm was employed.

C. Experiment 1: Analysis of the work done to move the foot over terrain A:

This experiment was conducted over the wood brick covered with black plain paper. It aimed to analyzed 1) the work required to slide the foot over a relatively smooth terrain for the configurations in Table III; therefore, position and force were collected for 30 trials for each combination 2) the evolution of the forces, position, and angles during slipping. Where 60 samples of the transient state, illustrated in Figure 5, from the 30 trials were extracted.

TABLE III

EXPERIMENTAL FEET CONFIGURATIONS. IN GENERAL, THE NOTATION $Hijk\_stiffness$ DENOTES A HOOF WITH JOINTS i, j, k FREE TO MOVE AT A GIVEN STIFFNESS. HL DENOTES A HOOF WITH ALL JOINTS LOCKED. THE CONFIGURATION $H123\_15B$ DENOTES A HOOF WITH JOINTS 1, 2 AND 3 FREE TO MOVE AT STIFFNESS $0.15N/mm$, AND WITH THE BACK-END OF THE HOOF CONNECTED TO REPRESENT THE EFFECT OF THE SKIN AS SHOWN IN FIGURE 6.

Name	**Feet type**	**Free joints' name**	K_{id}	**Back ends state**
ROUNDED	Rounded	-	-	free
HL	Hoof	-	-	free
H2	Hoof	2	-	free
H3	Hoof	3	-	free
H12_15	Hoof	1,2	0.15 N/mm	free
H123_5	Hoof	1,2,3	0.05 N/mm	free
H123_15	Hoof	1,2,3	0.15 N/mm	free
H123_55	Hoof	1,2,3	0.55 N/mm	free
H123_15B	Hoof	1,2,3	0.15 N/mm	linked

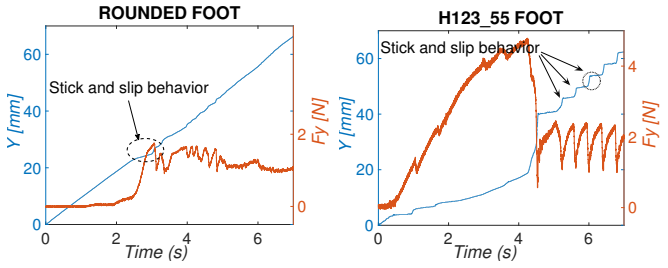

(a) (b)

Fig. 5. Position and force in the Y axis measured over the smooth terrain for the configuration: a) ROUNDED: position presents a minimum stick slip behavior when the foot is moved along the width of the tested distance and its maximum force is lower than that of hoof. b) H123_55: the stick and slip behavior is notoriously bigger than the previous described configuration; as a result, it has a higher maximum force value. Based on these information we can state that the work required to slip the foot is going to be higher for the second configuration.

D. Experiment 2: Analysis of the work done to move the feet over a terrain B:

The goal of this test was to analyzed the effect of the relatively high friction coefficient over the work required to slide the foot for the configurations presented in Table III. The number of trials collected was also 30 trials, as in Experiment 1. Nevertheless, this terrain was not used for the analysis during the transient because there was not enough evidence to prove that the data was statistically different. A deeper explanation is presented in Section IV-A.

E. Sensing

Position data was collected at 150 samples per second using the VICON motion capture system with 4 Bonita B10 cameras(250fps, 1 megapixels). 3 markers with radius of 6.4mm were attached to each object to obtain the position information. The objects were the claws, the rounded foot, and the reference in the rigid leg. VICON data acquisition process was carried out using MATLAB R2015b from MathWorks. In addition, the force was measured at the end of the rigid leg using the MINI40 SI-40-2 sensor with a sampling frequency of 900Hz. This information was gathered using LabView2010 from National Instruments.

F. Data Analysis

The data was analyzed using MATLAB R2015b. For the statistical analysis of the work the Statistics and Machine Learning Toolbox were utilized. Since the raw force data contained noise, it was filtered using the Wavelet toolbox (The Math Works Inc). Previous studies [14], [15] used the Mexican hat and Daubechies family (Db6), respectively, to analyze the frictional force. Nevertheless, in this paper the discrete wavelet transform was employed. Therefore, the Mexican hat was not taken into account because it is neither orthogonal nor biorthogonal. Criteria for selecting Haar wavelet with a decomposition level of 3 as a filter were as follows: the wavelet family was chosen based on the energy percentage that represents the data for all the samples where the low boundary for this energy was set to 97%; and, the decomposition level was selected depending on the highest energy corresponding to the details of the data using the previously selected wavelet.

IV. RESULTS AND DISCUSSION

We conducted 2 experiments with two feet whose shape and joints stiffness were modified according the 9 configurations in Table III. Our aims were to define the effect of morphological computation on: *A)* the work required to slip and *B)* the evolution of the displacement, forces, relative position of the tip and back end of the toes, and *C)* angles in the transient state to interpret their effect on the stability. To achieve our goals, the measured variables were force and position. Figure 5 illustrates raw data of position and force in the Y axis of the ROUNDED and H123_55 configurations for the smooth terrain. As can be seen, there is an stick and slip behavior that is more noticeable on the hoof than in the rounded foot because of the adaptability to the environment of the former. This increases the work required to slide this feet.

A. Analysis of the work required to slip

For the 30 trials of each configuration, the work required to slide the feet over the width of a smooth and relatively rough brick was calculated using Equation (12) and summarized in Figure 6.

$$W = \int_a^b f(x)\delta(x), \tag{12}$$

where W is the work in [N.mm], f is the force in Newtons, and x is the position in mm. Figure 6(a) illustrates that the average work required to move the rounded foot over the smooth terrain A was 61.6595 [N.mm], whereas hoofed configurations required between 191.79 [N.mm] and 223.2 [N.mm]. On the other hand, Figure 6(b) reveals that in terrain B the work needed for sliding the Rounded foot was on average 134.8342 [N.mm], while between 247.69 [N.mm] and 287.81 [N.mm] were needed for moving the hoof. For the statistical analysis, the data was normalized; however, the One-sample Kolmogorov-Smirnov test revealed that it was not normally distributed. Therefore, it was transformed using the

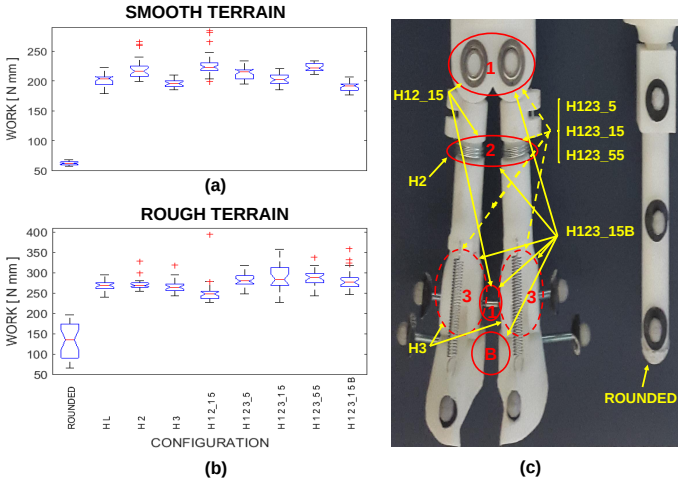

Fig. 6. Work in [N.mm] required to slip the feet over the terrains. Anova test revealed that work depends not only on the terrain and foot configuration but also on the interaction feet-terrain. Therefore, over a) the smooth terrain the work for the hoof was more than 3 times higher than that for the ROUNDED; additionally, the means of the configuration are different ($p<0.05$) which allows the analysis of the effect of the joints over the work. Similarly, in b) the rough terrain, whose coefficient of friction is higher than that of the smooth terrain, the work for the hoofed configuration was more than twice that of the ROUNDED foot. Nevertheless, there was not enough evidence to state that the means of the configuration were different. As a result, only the data of the smooth terrain was utilized for the analysis in the transient state.

logarithm. The Anova, anova n, reveals the important role of morphological computation on the work required to slip. This test indicated that work depends not only on the type of terrain and configuration but also on the interaction foot-terrain ($p<0.05$). Furthermore, the values for the same configuration but different terrain are statistically different ($p<0.05$).

To investigate the contribution of each joint, the data from each configuration within the same terrain was compared. However, for terrain B the work was mainly affected by the friction; therefore, there was not enough evidence to prove that the means were statistically different for some configurations. As a consequence, our analysis is based on the smooth terrain where the contributions of each joint for changing the work were more statistically differentiable. For analysis purposes, results were divided in the following 3 groups, depending on the number of locked joints and the stiffness of the interdigital spring and they were obtained using the MannWhitney U test with a ($p<0.05$) at the 1% significance level.

Group 1) ROUNDED, HL, H2, and H3: to discriminate the contribution of the joints, this group contains the configurations that have at most one free joint. Inside this group only for HL and H3 there is not enough evidence to state that their means are different from each other($p>0.05$); however, **H2** has the highest median and it is statistically different from the others ($p<0.05$). This suggest that friction between the pad and ground (measured in HL) is not the only factor that opposes to the movement. In this case joint 2 presents an important role for avoiding slipping.

Group 2) H12_15, H123_15, and H123_15B: to differentiate the effect of the interaction between joints, the common feature of these hoofed configurations is to have at lest 2 free joints at the same time. The statistical analysis demonstrates that all the means are different ($p<0.05$) and **H12_15** has the biggest median value. Nevertheless, as Figure 7(b) and Table IV reveal, the other configurations can have other features such as lower displacement and variability that also improve the stability.

Group 3) H123_5, H123_15, and H123_55: to comprehend the repercussion of the stiffness of the interdigital spring, it was changed to $K_{id} = 0.05N/mm$, $K_{id} = 0.15N/mm$, and $K_{id} = 0.55N/mm$, respectively. The analysis states that the medians are statistically different ($p<0.05$); and the highest work corresponds to **H123_55**. However, as stated before the work depends on the type of terrain; consequently, for terrain B it exhibits a direct relation with K_{id}, whereas for the smooth terrain it has a different behavior. Nevertheless, in both terrains the maximum value correspond to the highest k value.

To find the configuration with the highest work, H2, H12_15, and H123_55 were statistically compared, yet there was not enough evidence to state that they belong to different distributions. However, they have joint 2 in common that might be producing the highest slip dissipation.

B. Analysis of the position, forces, and relative positions during the transient for the hoofed configurations

In this section, we analyze the contribution of each joint on the improvement of the stability during the transient. However, data from the rough terrain and ROUNDED configuration was omitted because according the analysis of the previous section, averages of the distributions were not statistically different and the stick and slip behavior was almost at the minimum, respectively. Therefore, 60 samples that contain the slip and stick behavior from the 30 trials of the hoofed configurations over the smooth terrain were extracted. Their average, AVG, and standard deviation, SD, values are presented in Tables IV and V while their mean and standard errors are compared in 3 groups in Figure 7. It has to be pointed out that in this figure the intensity of the color increases with the work required to slide it. Besides, the data of *Group 1) HL, H2, and H3*; *Group 2) H12_15, H123_15, and H123_15B*; and *Group 3) H123_5, H123_15, and H123_55* is presented in columns while rows represent:

Row 1) Displacement y in the Y axis. It can be noticed that joint 2 contributes to the stabilization because H2 has not only the lowest displacement between all the configurations but also Table IV states that it has the lowest variability among all the groups. Moreover, the comparison of the displacement of H2 within the first group, Figure 7(a), indicates that these variables depend not only on the number of free joints but also on which one was unlocked. The second group, Figure 7(b), shows that the displacement increases with the degrees of freedom. In contrast, subfigure 7(c) shows that the displacement was minimally affected by the change of the stiffness of the K_{id} in Group 3. This result can be explained by the fact that the analysis in the previous subsection stated that the type of terrain has a significant influence; therefore in other

environments K_{id} can play a more influential role. A similar behavior is observed in subfigures 7(f), (i), and (l).

Row 2) Figures 7(d),(e), and (f) illustrate how morphological computation affects f_y. Therefore, subfigure (d) shows that the mean value is affected by the stiffness where HL has the highest value and H2 and H3 had the lowest value. Additionally, subfigures (e)(f) state that joint 3 also affects the rate of change of this force. Consequently, those configurations that include this joint present smoother profiles. This can be explained by the fact that some energy is stored in the antagonistic springs. Conversely, the same subfigures illustrate that the interaction of joints 2 and 1 increases the rate of change of f_y. This is also supported by Table IV that presents a high variability of this interaction that contrast with the low value of H2.

Row 3) On the other hand, subfigures 7(g), (h), and (i) support the relation between f_z and f_y presented in Equation 8 because when the feet are in contact with the ground, before 0.066 seconds and after the force generated by the interaction body environment stops its motion at 0.1 seconds, both variables have similar profiles.

Row 4) subfigures 7(j), (k), and (l) suggest that there is a link between y and β because when comparing the last and first row of Figure 7, the configuration with the highest values in displacement also has those of β.Additionally, the profiles of β state that the hoof tends to stands over the tips to avoid slipping.

TABLE IV
MEAN AND STANDARD DEVIATION OF Y[MM], f_y[N], AND f_z[N]

	y [mm]		f_y [N]		f_z [N]	
CONF.	**AVG**	**SD**	**AVG**	**SD**	**AVG**	**SD**
HL	1.758	0.315	1.734	0.124	4.273	0.356
H2	1.558	0.176	1.73	0.084	4.253	0.267
H3	1.652	0.209	1.585	0.135	4.254	0.261
H12_15	2.277	0.686	1.547	0.24	4.573	0.509
H123_5	1.998	0.441	1.622	0.174	4.246	0.39
H123_15	2.056	0.463	1.579	0.173	4.421	0.355
H123_55	2.084	0.42	1.628	0.149	4.241	0.389
H123_15B	1.874	0.318	1.377	0.206	4.542	0.34

C. Analysis of the angles during the transient for the hoofed configurations

As Table V presents, the value of the angles Θ, controlled by joint 1, and γ, controlled by joint 2, has a relatively low variability. Therefore, we chose only the configuration H123_55 to analyze the evolution of these variables. Figure 8 illustrates that the claw leaves the ground completely at 0.066 seconds. As a result, Θ increases the distance between the claws before this point to produce a larger slip dissipation orthogonal to the direction of walking. Thus, γ exhibits a decreasing behavior before 0.066 second which resembles the human behavior of turning the feet inward for avoiding slipping in an inclined surface. Consequently, γ will increase while the claws are in the air because it tries to reach is default position. After the feet reached the ground and stick at 0.1 seconds, both angles will change depending on the

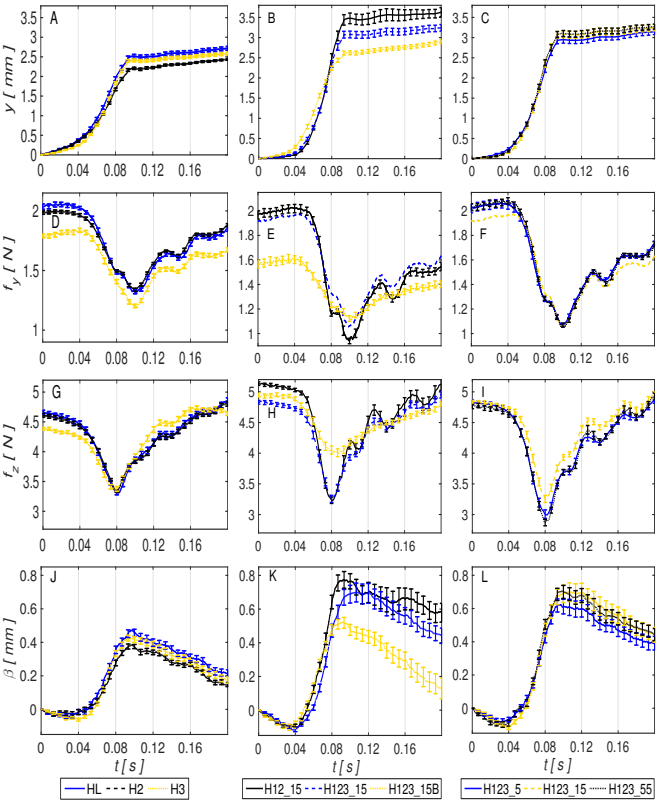

Fig. 7. Average and standard error of the data measured and calculated during the transient where the line color intensity is an indicator of the work presented in Figure 6. As a consequence, yellow, blue and black correspond to the lowest, medium and highest value, respectively. The data is presented in three columns and 4 rows. The first column contains the configuration that has at most one free joint, second column at least 2 free joints, and the last column a variation in the stiffness of the interdigital spring. *Row1:* presents the position y (a, b, c), (b)*Row2:* force f_y (d, e, f) along the Y axis; *Row3:* force f_z (g, h, i) along the Z axis; and *Row4:* the relative position β (j, k, l) of the tip with respect to the rear part of the toe.

roughness of the terrain to improve the contact area between the foot and ground. Moreover, the hoof was stable during the experiments because Θ never reached the critical value illustrated in Figure2(b). This can be a result of the lack of big irregularities on the terrains.

TABLE V
AVERAGE AND STANDARD DEVIATION OF Θ, γ, AND THE POSITION OF THE FRONTAL END OF THE CLAW WITH RESPECT TO ITS BACK END (β).

	Θ [◦]		γ [◦]		$\beta[mm]$	
CONF.	**AVG**	**SD**	**AVG**	**SD**	**AVG**	**SD**
HL	4.586	0.0173	65.48	0.162	0.224	0.144
H2	4.58	0.0224	62.328	0.172	0.179	0.102
H3	10.11	0.0172	57.756	0.099	0.573	0.197
H12_15	9.894	0.1807	60.879	0.319	0.199	0.114
H123_5	10.98	0.6793	61.023	0.333	0.423	0.316
H123_15	9.731	0.2204	61.636	0.308	0.317	0.275
H123_55	9.463	0.0347	61.874	0.279	0.355	0.226
H123_15B	6.744	0.0678	52.332	0.193	0.229	0.265

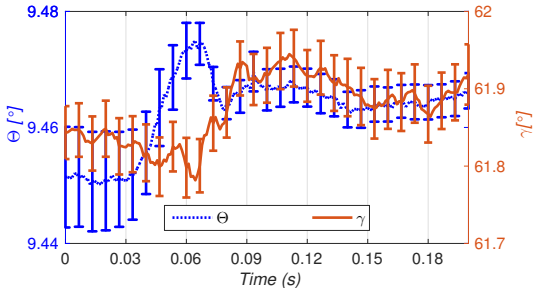

Fig. 8. Evolution of Θ and γ during the transient for the H123_55 configuration. (a) Θ increases before sliding at 0.066 seconds to increase the slip dissipation orthogonal to the movement direction. Conversely, (b) γ decreases before 0.066 seconds. While the hoof is in the air, both angles tend to recover their default position. Therefore, γ decreases while γ increases. Nevertheless, after reaching the ground both angles changed to improve the contact area between the foot and ground until t= 0.15 seconds where γ tends to increases again.

V. Conclusion

This paper for the first time shows how the morphological computation contributes to increase the work required to slide a foot along certain distance and affects the displacement, forces, relative position, and angles during the transient without affecting the power consumption and control complexity. The results of this study indicate that each joint plays a different role which depends not only of the number of unlocked joint but also on the environment. Therefore, these findings can be applied in robots for all terrain conditions to improve their stability without affecting other critical variables. In the future, the hoof should be tested in legged locomotion with punctuated collision forces in unstructured terrain conditions.

References

[1] N. Thrishantha, K. Byl, H. Liu, X. Song, and T. Villabona. "Dominant sources of variability in passive walking." In 2012 IEEE International Conference on Robotics and Automation (ICRA), pp. 1003-1010. IEEE, 2012.

[2] M. Raibert, Legged robots that balance. Vol. 3. Cambridge, MA: MIT press, 1986.

[3] D. Wooden, M. Malchano, K. Blankespoor, A. Howardy, A. Rizzi, and M. Raibert. "Autonomous navigation for BigDog." In 2010 IEEE International Conference on Robotics and Automation (ICRA), pp. 4736-4741. IEEE, 2010.

[4] M. Murphy, A. Saunders, C. Moreira, A. Rizzi, and M. Raibert, The littledog robot, Int. J. Rob. Res., pp. 1-5, 2010.

[5] A. S. Boxerbaum, J. Oro, G. Peterson, and R. D. Quinn, The latest generation Whegs^{TM}robot features a passive-compliant body joint, in Intelligent Robots and Systems, 2008. IROS 2008. IEEE/RSJ International Conference on, 2008, pp. 1636-1641.

[6] U. Saranli, RHex: A Simple and Highly Mobile Hexapod Robot, Int. J. Rob. Res., vol. 20, pp. 616-631, 2001.

[7] M. M. Dalvand and M. M. Moghadam, Stair climber smart mobile robot (MSRox), Auton. Robots, vol. 20, pp. 3-14, 2006.

[8] J. B. Jeans and D. Hong, IMPASS: Intelligent Mobility Platform with Active Spoke System, 2009 IEEE Int. Conf. Robot. Autom., pp. 1605-1606, 2009.

[9] D. N. Beal, F. S. Hover, M. S. Triantafyllou, J. C. Liao, and G. V. Lauder, "Passive propulsion in vortex wakes", J. Fluid Mech., vol. 549, pp. 385-402, 2006.

[10] D. H. Chadwick, A beast the color of winter: the mountain goat observed, Bison Book. University of Nebraska Press, 2002.

[11] N. Jamal, Y. Mazaheri, and U. K. Mohabady, Gross anatomy of the ligaments of fetlock joint in dromedary camel, Journal of Camel Practice and Research, 18.2, pp. 197-202, 2011.

[12] DYCE, K.M.; SACK, W.O.; WENSING, C.J.G., Miembros locomotores del cerdo, in Anatomia Veterinaria, 3th ed, Mexico: Elsevier, 2007, pp. 875-878.

[13] G. Constantinescu, Guide to Regional Ruminant Anatomy Based on The Dissection of The Goat, 1rst ed, Wiley, 2001, Fig. 2.10.

[14] Chen, C., Kovacevic, R., and Jandgric, D. Wavelet transform analysis of acoustic emission in monitoring friction stir welding of 6061 aluminum. International Journal of Machine Tools and Manufacture, Vol. 43, no.13, pp. 1383-1390, 2003.

[15] Naerum, E., Cornella, J., and Elle, O. J. Wavelet networks for estimation of coupled friction in robotic manipulators. In Robotics and Automation, 2008. ICRA 2008. IEEE International Conference on, pp. 862-867, May 2008.